AOC, A BEAM DYNAMICS DESIGN CODE FOR MEDICAL AND INDUSTRIAL ACCELERATORS AT IBA

W. Kleeven*, M. Abs, E. Forton, V. Nuttens, E. Pearson, J. Van de Walle, S. Zaremba
Ion Beam Applications (IBA), Louvain-la-Neuve, Belgium

Abstract

The Advanced Orbit Code (AOC) facilitates design studies of critical systems and processes in medical and industrial accelerators. Examples include: i) injection into and extraction from cyclotrons, ii) central region, beam-capture and longitudinal beam dynamics studies in synchro-cyclotrons, iii) studies of resonance crossings, iv) stripping extraction, v) beam simulation from the ion source to the extraction, vi) space charge effects, vii) beam transmission studies in gantries or viii) calculation of Twiss-functions. The main features of the code and some applications are discussed.

ILLUSTRATION OF THE FEATURES

AOC tracks accelerator orbits under the combined action of static magnetic and RF electric fields, using time as independent variable. Table 1 shows the most important features.

Different accelerators and magnet systems can be handled such as i) isochronous cyclotrons, ii) synchro-cyclotrons, iii) Rhodotrons [1], iv) FFAG's and v) particle therapy gantries.

The equations of motion are integrated by a 5th order Runge-Kutta with adaptive step-size control. This results in high precision and facilitates the tracking of an accelerator from the ion source up to the beam extraction. Three types of motion can be integrated: i) 3D particle trajectories ii) Twiss optical functions with respect to a planar orbit and iii) the 3D design orbit of a cyclotron spiral inflector.

For the first type, space charge (SC) effects can be included. The fully relativistic and fully 3D electric and magnetic self-fields are calculated for a bunch in free space, by acummulating for each particle the contributions of all others. For SC, a single step, or a more precise converging iterative solution can be chosen. To test the SC option, a space-charge dominated 50 keV zero-emittance electron bunch was tracked in a drift and the rms-envelopes were compared with theoretical 3D envelope equations [2]. Two cases were studied: i) a spherical bunch with a diameter of 10 mm and a local peak current of 28 A and ii) a long (cigar-shape) bunch with a diameter of 10 mm, a length of 200 mm and a local peak current of 14 A. Fig. 1 shows an almost perfect fit between the theoretical (solid lines) and AOC (markers) calculations.

The code uses multi-threading in order to speed up calculations. Fig. 2 shows a typical performance for a SC calculation on a standard work station having 24 logical processors. It is seen that a gain with a factor of about 13 is obtained.

There are two ways to import the static magnetic field map of a magnet into AOC. The first method assumes that the field is specified on a 2D plane and first or higher order field

Table 1: AOC Features

SCOPE OF APPLICATIONS
Cyclotrons (isochronous, synchronous)
FFAG's, Rhodotrons, PT-gantries
Static magnetic fields, RF and/or static electric fields
EQUATIONS OF MOTION SOLVED
3D-trajectories, Twiss-functions, inflector design orbits
INTEGRATION METHOD
Time domain, Runge-Kutta 5th order, adaptive step
SPACE CHARGE CALCULATIONS
Fully relativistic, fully 3D centroids
E- and B-self fields, iterative or single-step solution
OTHER IMPORTANT FEATURES
Cyclotron injection (axial, internal source)
Cyclotron extraction (stripping, ESD), Multi-threading
Detection of beam-losses, orbit back-tracking
Choice between cartesian and polar coordinate systems
Application of angular kicks, Dee-voltage ripple
MAGNETIC AND ELECTRIC FIELD INPUT
Linear or non-linear expansion from 2D B-maps
3D B-maps of multiple magnets on multiple grids
3D E-maps on multiple grids, or simplified dee-gaps
POST-PROCESSING OPTIONS
Beam rms-analysis, radial probe tracks
patch intersections, cyclotron Smith-Garren analysis

expansion is used to obtain the field outside of this plane. Such 2D maps can be obtained from measurements or from magnet calculations. For higher (third) order expansion, also the 2D Laplacian in the 2D plane needs to be given. Also median plane errors can be specified in the same plane.

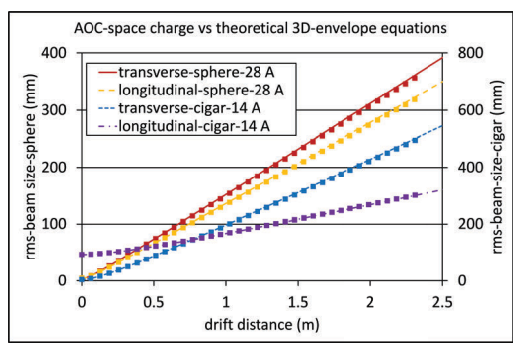

Figure 1: Bench-marking of the SC module in AOC.

In the second method, the full 3D field components are specified on a 3D grid and the fields are calculated by Lagrange polynomial interpolation. The degree of interpolation is a free parameter. The full 3D grid may consist

* willem.kleeven@iba-group.com

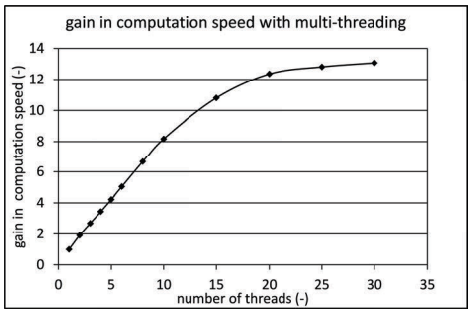

Figure 2: Illustration of the efficiency of multi-threading.

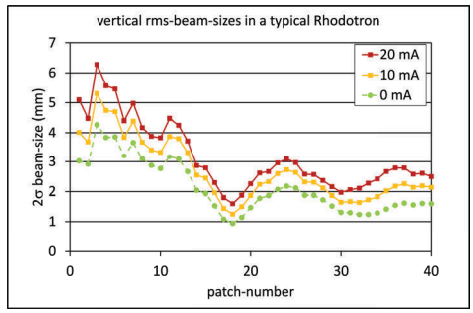

Figure 4: Vertical rms beam-sizes as calculated with space charge in a typical Rhodotron for different beam currents.

of multiple 3D meshes each with different topology. This allows to zoom in on details which need finer mesh then elsewhere. Exactly the same approach is used for the 3D electrical field maps. The RF electric field may be generated from different sources with different RF-frequencies (including DC), RF-phases and electrode voltages. There is also a possibility to calculate electric field maps from a simplified dee-geometry (using Gaussian profiles expanded around straight gaps) if 3D maps are not available. Various rotational and reflection symmetries of field-maps are supported. For magnetic structures, there is also a possibility to import multiple magnets, each specified on a single mesh. In this case AOC allows to position and orientate each magnet with 5 degrees of freedom. The 3D field-maps can be obtained from 3D finite element packages such as Opera3D [3].

Fig. 3 shows a space-charge beam in a typical industrial Rhodotron [1]. This accelerator consists of a coaxial RF cavity around which a number of magnetic dipoles are placed that, after a passage of the electron beam through the cavity, re-inject into the cavity for the next passage. There are 10 passages with an energy gain of 1 MeV per passage. The beam with an average current of 10 mA (roughly 100 mA peak in the bunch) is calculated self-consistently starting from the 35 kV electron gun up to extraction. The cavity RF mode is TEM and also can be calculated with Opera3D.

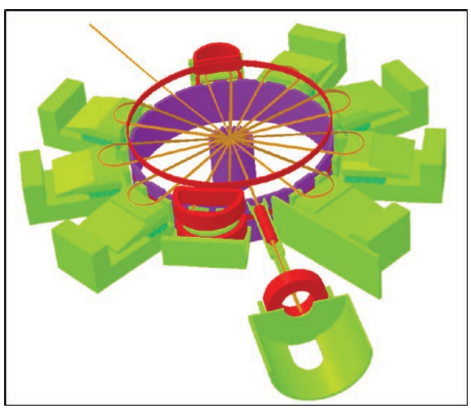

Figure 3: Space charge simulation of a Rhodotron.

Fig. 4 shows for the same Rhodotron example, the vertical rms beam sizes (for average beam currents of 0, 10 and 20 mA) along the 10 passes and sampled 4 times each pass. A current of 10 mA can be accelerated without any beam-losses.

Fig. 5 shows an example of a central region design for an isochronous PET cyclotron with internal ion source. The calculation starts at the aperture slit of the source. The 3D electric field is obtained from an Opera3D electrostatic calculation. This is allowed if the geometry is small compared to the RF wavelength. Full dee-structures can also be handled by AOC, and in this case the dee-voltage profile with radius is adjusted if needed, based on a 3D self-consistent RF finite-element modeling of the structure. Important design goals for a cyclotron central region are i) good horizontal and vertical beam centering, ii) good vertical electric focusing and iii) good beam transmission. AOC is able to monitor beam losses on RF electrodes or magnetic iron. This is based on material labels included in the 3D field input files. AOC also allows to program mathematically 3D geometries that may intercept particles.

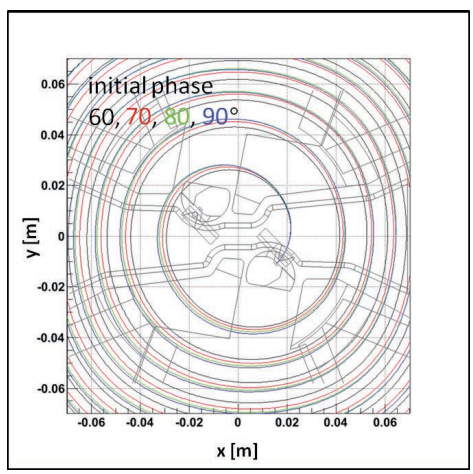

Figure 5: Central region of the c18-twin 18 MeV PET isotope production cyclotron. Four simulated orbits with different RF starting phases are superimposed on the design geometry. There are two internal ion sources placed at 180 deg.

Another application is the design of cyclotron axial injection. Fig. 6 shows the simulation of a spiral inflector [4]. AOC allows to calculate the complex 3D orbits with space

ISBN 978-3-95450-147-2

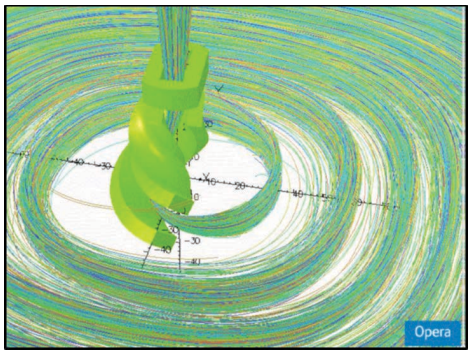

Figure 6: Simulation of the axially injected beam through a spiral inflector into a 30 MeV medical cyclotron.

charge. The difficulty is to find the centroid of the inflector in the varying 3D magnetic field. A special set of equations of motion is integrated, in which the static inflector electric field is all the time perpendicular to the orbit. An automatic iteration optimizes the inflector parameters such that the orbit is injected perfectly onto the median plane and also perfectly on the accelerated equilibrium orbit. Once this orbit is known, the inflector design becomes relatively simple.

In synchro-cyclotrons, the frequency as well as the voltage of the RF are modulated in time in order to ensure resonant acceleration up to beam extraction. There is a longitudinal beam dynamics as in synchrotrons and the beam can only be captured during a short time-window. This process has been studied, for the IBA superconducting synchro-cyclotron S2C2 [5] and a result is shown in Fig. 7. A large number of particles is lauched in the cyclotron center at the moment where the RF frequency is not far off from the revolution frequency, with starting RF phases and starting times uniformly distributed between 0 deg and 90 deg and 30 μs and 40 μs respectively. The upper of Fig. 7 shows the longitudinal phase acceptance indicated by black dots. The colouring zones in the lower figure show how the filling of the separatrix is related to the starting times: early particles are close the phase space center (near the synchronous particle) and late particles end up close to the separatrix.

Three cyclotron extraction schemes are available: i) by stripping of H^- or H_2^+; multiple stripper foils can be placed simultaneously, ii) with an electrostatic deflector (ESD) where the electric field of the ESD is replaced locally by a drop in magnetic field and iii) with an ESD for which the electric field is specified in a full 3D map. Fig. 8 shows a simulation of dual stripping extraction in a 18 MeV medical cyclotron. The accelerated beam can be evenly distributed on two oppositely placed isotope production targets.

AOC can integrate Twiss-parameters along a median plane orbit. This has allowed for example, the optical design and matching of extraction systems, without the need to immediately rely on elaborate 3D particle tracking. Furthermore there are several tools in AOC, to process the calculated beam. An example of a radial probe track is shown in Fig. 9. The differential signal shows the pattern of the separate turns. The integral signal shows the beam transmission.

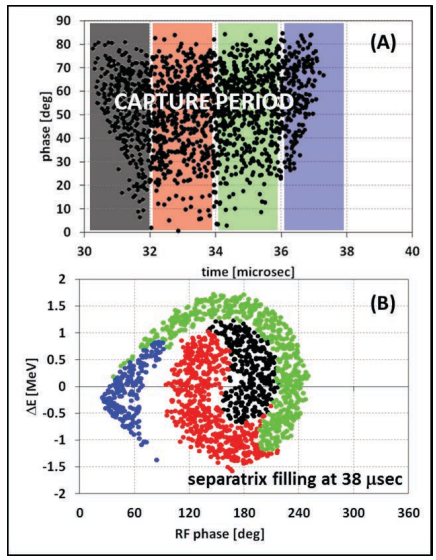

Figure 7: Simulation of beam capture in a synchro-cyclotron.

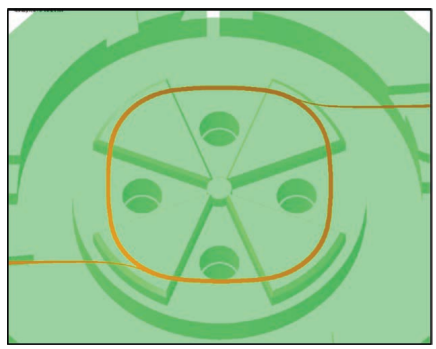

Figure 8: Example of dual beam stripping extraction.

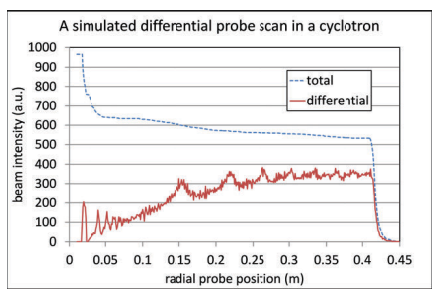

Figure 9: Simulation of a cyclotron differential probe.

REFERENCES

[1] J. M. Bassaler *et al.*, "Rhodotron: an accelerator for industrial irradiation", *Nucl. Instr. Meth.*, vol. B68, pp. 92–95, 1992.

[2] F. J. Sacherer, "rms envelope equations with space charge", *IEEE Trans. Nucl. Sci.*, vol. 18, pp. 1105–1107, 1971.

[3] Cobham, `http://http://operafea.com`

[4] J. L. Belmont and J. L. Pabot, "Study of Axial Injection for the Grenoble Cyclotron", *IEEE Trans. Nucl. Sci.*, vol. NS-13, pp. 191–193, 1966.

[5] W. Kleeven *et al.*, "The IBA superconducting synchrocyclotron project S2C2"' in *Proc. 20st Int. Conf. Cycl. Appl.*, Vancouver, Canada, September 2013, paper MO4PB02, pp. 115–119.